

# Vector Quantized Diffusion Model with CodeUnet for Text-to-Sign Pose Sequences Generation

Pan Xie  
Beihang University  
panxie@buaa.edu.cn

Zexian Li  
Beihang University  
lizexian0427@gmail.com

Qipeng Zhang  
Beihang University  
zhangqipeng@buaa.edu.cn

Yao Du  
Beihang University  
duyao@buaa.edu.cn

Hao Tang  
CVL, ETH Zurich  
haotang@vision.ee.ethz.ch

Xiaohui Hu  
Chinese Academy of Sciences  
hxh@iscas.ac.cn

## Abstract

*Sign Language Production (SLP) aims to translate spoken languages into sign sequences automatically. The core process of SLP is to transform sign gloss sequences into their corresponding sign pose sequences (G2P). In this paper, we propose a novel paradigm to realize this pose sequence generation task. Specifically, we transform the continuous pose space generation problem into a discrete space sequence generation problem: 1) we introduce Pose-VQVAE, a new framework that combines VAEs with vector quantization to obtain a discrete latent representation for the continuous pose sequence. 2) we model the latent prior by proposed PoseVQ-Diffusion, which is a denoising diffusion architecture for length-varied discrete sequence data. Besides, we propose a CodeUnet model to better leverage the spatial-temporal information for generating higher-quality pose sequences in discrete space. Moreover, we develop a heuristic sequential clustering method to predict the variable lengths of pose sequences for corresponding gloss sequences. Consequently, compared with previous state-of-the-art G2P models, our model achieves significantly better performance on the public SLP evaluation benchmark. More generated results can be found on the project page [https://slpdifusier.github.io/slp\\_vqdiffusion](https://slpdifusier.github.io/slp_vqdiffusion).*

## 1. Introduction

Sign Language Production (SLP), as an essential task for the Deaf community, aims to provide continuous sign videos for spoken language sentences. Since sign languages are distinct linguistic systems [28] which differ from natural languages, sign languages have different word orders from their corresponding natural languages. Therefore, directly learning the alignment mapping between them is challenging.

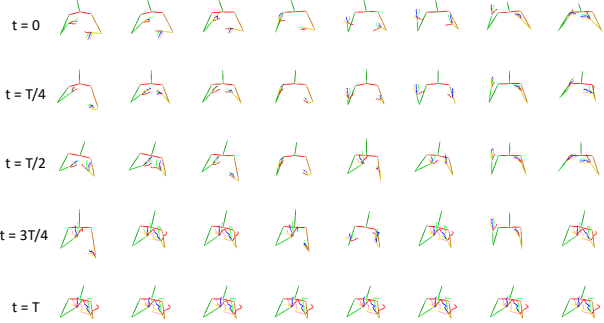


Figure 1. The forward diffusion process applied to a pose sequence. The first line ( $t=0$ ) is the original pose sequence. The remaining four lines represent the noised discrete sequence decoded by PoseVQVAE. For readability, we select one frame every three frames for a total of 8 frames, and we set  $T = 100$  in this example.

To tackle this issue, previous works first translate spoken languages into glosses<sup>1</sup>, then generate the sign pose sequences based on the gloss sequences (G2P) [31, 33], and finally optionally use the sign pose sequence to generate the photo-realistic sign video [32]. Accordingly, G2P is the heart procedure of this task, and it is the focus of this paper.

Existing methods for G2P can be categorized into autoregressive [31, 33] and non-autoregressive [20] depending on their decoding strategies. Autoregressive models [31, 33] generate the next pose frame depending on previous frames relying on the teacher forcing strategy [41]. In inference, the recurrent decoding is likely to lead to prediction error propagation over time due to the exposure bias [35]. To break the bottleneck of autoregression, non-autoregressive methods are proposed to induce the decoder to generate all target predictions simultaneously [13, 14]. Huang *et al.* [20] proposed a non-autoregressive G2P model to generate sign pose

<sup>1</sup>Sign glosses are spoken language words that match the meaning of signs and, linguistically, manifest as minimal lexical items.

sequence parallelly in a one-shot decoding scheme and used an External Aligner (EA) for sequence alignment learning.

Motivated by the recently developed Discrete Denoising Diffusion Probabilistic Model (D3PMs) [2, 15, 18] which achieved impressive results for language generation and vector quantized image generation. In this paper, we propose a two-stage method to transform the continuous pose sequence into discrete tokens and model the discrete prior space with the recently developed denoising diffusion architecture. It is an iterative non-autoregressive method that performs parallel refinement on the generated results and therefore shows expressive generative capacity.

We elaborate our approach in three steps. Firstly, we utilize a vector quantized variational autoencoder (VQ-VAE) to represent the pose sequence as sequential latent codes. Unlike image VQ-VAE [12, 39], we devise a specific architecture, Pose-VQVAE, to learn the meaningful latent embedding space by reconstructing the pose sequence. Specifically, we divide a sign skeleton into three local point patches representing pose, right hand, and left hand separately. Furthermore, we utilize a multi-codebook to maintain separated latent embedding space for different local patches. As a result of stronger feature semantics, we ease the difficulty in constructing mappings between the sign pose feature and the codebook feature, thus improving the reconstruction quality.

Next, we extend the standard vector quantized diffusion methods [2, 15] to model the sequential alignments between sign glosses and quantized codes. The discrete diffusion model samples the data distribution by reversing a forward diffusion process that gradually corrupts the input via a fixed Markov chain. Its corruption process by adding noise data (*e.g.*, [MASK] token) draws our attention to the mask-based generative model, Mask-Predict [13], which is proved to be a variant of diffusion model [2]. In this paper, we explore two variants of the diffusion model for our variable-length sequence generation. To better leverage the spatial and temporal information of the quantized pose sequences, we introduce a new architecture CodeUnet. In contrast to Unet [30], which is a “fully convolution network” for image data, CodeUnet is a “fully transformer network” designed for discrete tokens. As a result of iterative refinements and better spatial-temporal modeling, our model achieves a higher quality of conditional pose sequence generation.

Lastly, the length prediction of the non-autoregressive G2P models is challenging since the corresponding lengths of different sign glosses are different and variable. In this paper, we propose a novel clustering method for this specific sequential data that local adjacent frames should belong to a cluster. Specifically, taking advantage of the meaningful learned codes in the first stage, we apply the k-nearest-neighbor-based density peaks clustering algorithm [11, 45] to locate the peaks with higher local density. Secondly, we design a heuristic algorithm to find the boundary between

two peaks according to their semantic distance with the two peak codes. Finally, we leverage the length of each gloss as the additional supervised information and predict the length of the gloss sequence in the inference.

Our model significantly improves the generation quality on the challenging RWTH-PHOENIX-WEATHER-2014T [5] dataset. The evaluation of conditional sequential generation is evaluated using a back-translated model. Extensive experiments show that our model increases the WER score from 82.01% [20] to 77.26% on generated pose sequence to gloss sequence, and BLEU score from 6.66 [20] to 7.50 on generated pose sequence to spoken language.

## 2. Related Works

**Sign Language Production.** Most sign language works focus on sign language recognition (SLR) and translation (SLT) [5–7, 19, 43, 46], aiming to translate the video-based sign language into text-based sequences. And few attempts have been made for the more challenging task of sign language production (SLP) [38, 42]. Stoll *et al.* proposed the first deep SLP model, which adopts the three-step pipeline. In the core process for G2P, they learn the mapping between the sign glosses and the skeleton poses via a look-up table. After that, B. Saunders *et al.* [33] proposed the progressive transformer to learn the mapping with an encoder-decoder architecture and generate the sign pose in an autoregressive manner in the inference. Further, B. Saunders *et al.* [32] proposed a Mixture Density Network (MDN) to generate the pose sequences condition on the sign glosses and utilize a GAN-based method [9] to produce the photo-realistic sign language video. B. Saunders *et al.* [34] translated the spoken language to sign language representation with an autoregressive transformer network and used the gloss information to provide additional supervision. Then they proposed a Mixture of Motion Primitives(MoMP) architecture to combine distinct motion primitives to produce a continuous sign language sequence.

Different from these autoregressive methods, Huang *et al.* [20] proposed a non-autoregressive model to parallelly generate the sign pose sequence avoiding the error accumulation problem. They applied the monotonic alignment search [23] to generate the alignment lengths of each gloss. Our model also explores a non-autoregressive method with a diffusion strategy, and the adopted diffusion model architecture allows us to refine the results with multiple iterations.

**Denoising Diffusion Probabilistic Models.** Diffusion generative models have achieved outstanding results on continuous data, such as image generation [10, 16, 17, 26, 29] and speech synthesis [21, 22, 24]. However, most previous works focus on Gaussian diffusion processes that operate in continuous state spaces. The discrete diffusion model is first introduced in [36], and it is applied to text generation in Argmax Flow [18]. To improve and extend the discrete

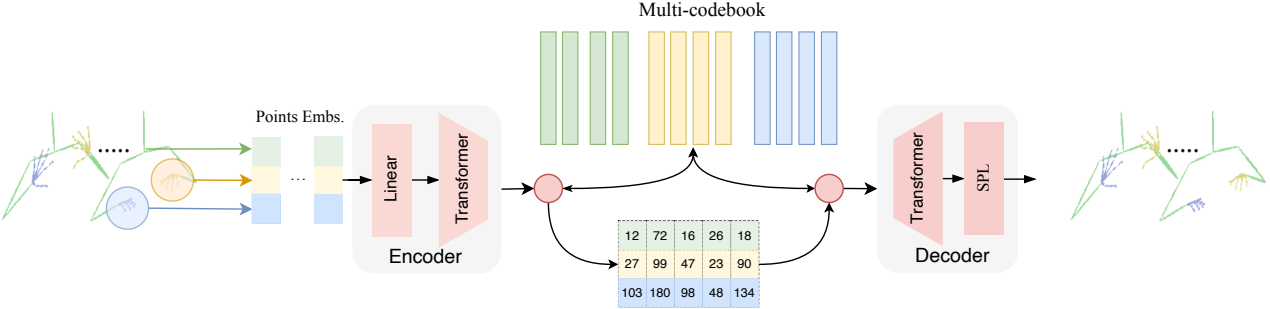


Figure 2. The architecture of the first stage model Pose-VQVAE for learning the discrete latent codes.

diffusion model, D3PM [2] used a structured categorical corruption process to shape data generation and embed structure in the forward process. VQ-Diffusion [15] applied the discrete diffusion model to conditional vector quantized image synthesis with a mask-and-replace diffusion strategy. Upon this work, we extend this diffusion strategy with more special states to length-varied discrete sequence data and introduce an Unet-like “fully transformer” network to model spatial-temporal space.

### 3. The Proposed Method

This paper aims to extend the discrete diffusion model for conditional sign pose sequence generation. The proposed PoseVQ-Diffusion model consists of three key components, i.e., the Pose-VQVAE to learn the latent codes, a discrete diffusion model with CodeUnet to model the discrete codes generation, and a sequential-KNN algorithm on the length prediction for this non-autoregressive method.

#### 3.1. Pose VQ-VAE

In this section, we introduce how to tokenize the points of a sign pose skeleton into a set of discrete tokens. A naive approach is to treat per point as one token. However, such a points-wise reconstruction model tends to have tremendous computational cost due to the quadratic complexity of self-attention in Transformers. On the other hand, since the details of hand points are essential for sign pose understanding, treating all the points into one token leads to remarkably inferior reconstruction performance. To achieve a better trade-off between quality and speed, we propose a simple yet efficient implementation that groups the points of a sign skeleton into three local patches, representing pose, right hand, and left hand separately. Figure 2 illustrates the framework of our proposed Pose-VQVAE model with the following submodules.

**Encoder.** Given a sign pose sequence of  $N$  frames  $\mathbf{s} = (s_1, s_2, \dots, s_n, \dots, s_N) \in \mathbb{R}^{N \times J \times K}$ , where  $\{x_n^j\}_{j=1}^J$  presents a single sign skeleton containing  $J$  joints and  $K$  denotes the feature dimension for human joint data. We separate these points into three local patches,  $\mathbf{s}_p \in \mathbb{R}^{N \times (J_p \times K)}$ ,  $\mathbf{s}_r \in \mathbb{R}^{N \times (J_r \times K)}$ , and  $\mathbf{s}_l \in \mathbb{R}^{N \times (J_l \times K)}$  for the pose, right

hand, and left hand, respectively, where  $J = J_p + J_r + J_l$ . In the encoder module  $E(e|\mathbf{s})$ , we first transform these three point sequences into feature sequences by simple three linear layers and concatenate them together. Then we apply a spatial-temporal Transformer network to learn the long-range interactions within the sequential point features. Finally, we arrive at the encoded features  $\{e_n \in \mathbb{R}^{3 \times h}\}_{n=1}^N$ .

**Multi-Codebook.** Similar to image VQ-VAE [39], we take the encoded features as inputs and convert them into discrete tokens. Specifically, we perform the nearest neighbors method  $\mathcal{Q}(z|e)$  to quantize the point feature to the quantized features  $\{z_n \in \mathbb{R}^{3 \times h}\}_{n=1}^N$ . The quantized features are maintained by three separate codebooks, where each codebook is of size  $V$ .

**Decoder.** The decoder  $D(\tilde{\mathbf{s}}|z)$  receives the quantized features as inputs and also applies spatial-temporal Transformer to get the output features  $\{o_n \in \mathbb{R}^{3 \times h}\}_{n=1}^N$ . Finally, we separate the output feature for three sub-skeleton and utilize a structured prediction layer (SPL) [1]  $\mathcal{P}(\tilde{\mathbf{s}}|o)$  to reconstruct the corresponding sub-skeleton  $\tilde{\mathbf{s}}_p \in \mathbb{R}^{N \times (J_p \times K)}$ ,  $\tilde{\mathbf{s}}_r \in \mathbb{R}^{N \times (J_r \times K)}$ , and  $\tilde{\mathbf{s}}_l \in \mathbb{R}^{N \times (J_l \times K)}$ . We adopt the SPL to rebuild the skeleton from feature because it explicitly models the spatial structure of the human skeleton and the spatial dependencies between joints. The hierarchy chains of the pose, right hand, and left hand skeleton are given in the Appendix.

**Training.** The encoder  $E(e|\mathbf{s})$ , tokenizer  $\mathcal{Q}(z|e)$ , and decoder  $D(\tilde{\mathbf{s}}|z)$  can be trained end-to-end via the following loss function:

$$\mathcal{L}_{\text{Pose-VQVAE}} = \|\mathbf{s}_p - \tilde{\mathbf{s}}_p\| + \|\mathbf{s}_r - \tilde{\mathbf{s}}_r\| + \|\mathbf{s}_l - \tilde{\mathbf{s}}_l\| + \|\text{sg}[e] - z\| + \beta \|\text{sg}[z] - e\|, \quad (1)$$

where  $\text{sg}[\cdot]$  stands for stop-gradient operation.

#### 3.2. Discrete Diffusion Model with CodeUnet

To allow conditional sampling, a discrete diffusion model is trained on the latent codes obtained from the Pose-VQVAE model. Figure 3 shows the architecture of our proposed PoseVQ-Diffusion, which aims to model the latent space

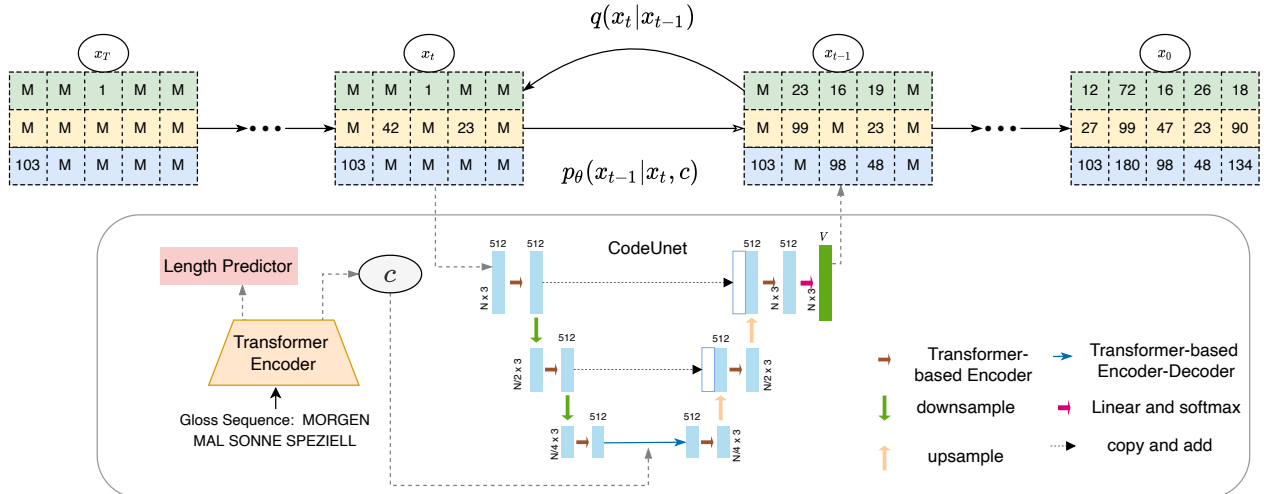


Figure 3. Our approach uses a discrete diffusion model to represent the Vector-Quantized sign pose sequence allowing non-autoregressive pose sequence generation. Specifically, after compressing the sign pose sequences to meaningful discrete codes, each code is randomly masked or replaced, and a CodeUnet model is trained to restore the original data.

in an iterative non-autoregressive manner. We will subsequently introduce the diffusion process, reverse denoising process, and the parameterized model CodeUnet.

**Diffusion Process.** Given a sequence of latent codes  $x_0 \in \mathbb{R}^{N \times 3}$  obtained from the vector quantized model, where  $x_0^{(i,j)} \in \{1, 2, \dots, V\}$  at location  $(i, j)$  represents the index within the codebook. The diffusion process aims to corrupt the original data  $x_0$  via a fixed Markov chain  $p(x_t|x_{t-1})$  by adding a small amount of noise continuously. After a fixed  $T$  timesteps, it produces a sequence of increasingly noisy data  $x_1, \dots, x_T$  with the same dimensions as  $x_0$ , and  $x_T$  becomes a pure noise sample.

For the scalar discrete variables with  $V$  categories  $x_t^{(i,j)} \in [1, V]$ , the forward transition probabilities from  $x_{t-1}$  to  $x_t$  can be represented by matrices  $[Q_t]_{mn} = q(x_t = m|x_{t-1} = n) \in \mathbb{R}^{V \times V}$ . Note that we omit the superscripts  $(i, j)$  to avoid confusion. Then the forward diffusion process can be written as:

$$q(x_t|x_{t-1}) = \mathbf{x}_t^T Q_t \mathbf{x}_{t-1}, \quad (2)$$

where  $\mathbf{x}_t \in \mathbb{R}^{V \times 1}$  is the one-hot version of  $x_t$  and  $Q_t \mathbf{x}_{t-1}$  is the categorical distribution for  $x_t$ . A nice property of the above Markov diffusion process is that we can sample  $x_t$  as any timestep directly from  $x_0$  as:

$$q(x_t|x_0) = \mathbf{x}_t^T \bar{Q}_t \mathbf{x}_0, \text{ with } \bar{Q}_t = Q_t \dots Q_1. \quad (3)$$

D3PM [2] formulates the transition matrix  $Q_t \in \mathbb{R}^{V \times V}$  by introducing a small number of uniform noises to the categorical distribution. As formulated as the first matrix in Eq. (4) with  $\alpha \in [0, 1]$  and  $\beta_t = (1 - \alpha_t)/V$ . It can be interpreted as each token having a probability of  $\alpha_t + \beta_t$  to remain the previous value and a probability of  $\beta_t$  to be

the value from the whole  $V$  categories. Based on D3PM, VQ-Diffusion [15] proposes a mask-and-replace diffusion strategy that not only replaces the previous value but also inserts [MASK] token to explicitly figure out the tokens that have been replaced. We extend this mask-and-replace strategy to our variable-length sequence modeling. Since the length of pose sequences may be different in a minibatch, we have to add two special tokens, [MASK] and [PAD] tokens, so each token has  $V + 2$  states. The mask-and-replace diffusion process can be defined as follows: each token has a probability of  $\alpha_t$  to be unchanged,  $V\beta_t$  to be uniformly resampled, and  $\gamma_t = 1 - \alpha_t - V\beta_t$  to be replaced with [MASK] token. Note that [MASK] and [PAD] tokens always keep their own state. The transition matrix  $Q_t \in \mathbb{R}^{(V+2) \times (V+2)}$  is formulated as the second matrix of the following:

$$Q_t = \begin{bmatrix} \alpha_t + \beta_t & \beta_t & \dots & \beta_t & 0 & 0 \\ \beta_t & \alpha_t + \beta_t & \dots & \beta_t & 0 & 0 \\ \vdots & \vdots & \ddots & \vdots & \vdots & \vdots \\ \beta_t & \beta_t & \dots & \alpha_t + \beta_t & 0 & 0 \\ \gamma_t & \gamma_t & \dots & \gamma_t & 1 & 0 \\ 0 & 0 & \dots & 0 & 0 & 1 \end{bmatrix}; \quad (4)$$

$$Q_t = \begin{bmatrix} \alpha_t + \beta_t & \beta_t & \dots & \beta_t & 0 & 0 \\ \beta_t & \alpha_t + \beta_t & \dots & \beta_t & 0 & 0 \\ \vdots & \vdots & \ddots & \vdots & \vdots & \vdots \\ \beta_t & \beta_t & \dots & \alpha_t + \beta_t & 0 & 0 \\ \gamma_t & \gamma_t & \dots & \gamma_t & 1 & 0 \\ 0 & 0 & \dots & 0 & 0 & 1 \end{bmatrix}. \quad (5)$$

Finally, the categorical distribution of  $\mathbf{x}_t$  can be derived

as following using reparameterization trick:

$$\text{when } x_0 \neq V + 2, \quad \bar{Q}_t \mathbf{x}_0 = \begin{cases} \bar{\alpha}_t + \bar{\beta}_t, & x_t = x_0 \\ \bar{\beta}_t, & x_t \neq x_0 \text{ and } x_t \leq V \\ \bar{\gamma}_t, & x_t = V + 1 \\ 0, & x_t = V + 2 \end{cases}$$

$$\text{when } x_0 = V + 2, \quad \bar{Q}_t \mathbf{x}_0 = \begin{cases} 0, & x_t \neq V + 2 \\ 1, & x_t = V + 2 \end{cases} \quad (6)$$

where  $\bar{\alpha}_t = \prod_{i=1}^t \alpha_i$ ,  $\bar{\gamma}_t = 1 - \prod_{i=1}^t (1 - \gamma_i)$ , and  $\bar{\beta}_t = (1 - \bar{\alpha}_t - \bar{\gamma}_t)/V$ . Therefore, we can directly sample  $x_t$  within the computation cost  $O(V)$ . A visualized example of the diffusion process is shown in Figure 1, we first get the noised latent codes by  $q(x_t|x_t)$ , and decode them to sign skeleton with Pose-VQVAE decoder module.

**Reverse Denoising Process.** The reverse denoising process aims to recreate the real sample from a full noise input by gradually sampling from  $q(x_{t-1}|x_t)$ . However, it is intractable to estimate the conditional probability  $q(x_{t-1}|x_t)$  since it needs to use the whole dataset. Fortunately, the conditional probability is tractable when conditioned on  $x_0$  using Bayes' rule:

$$q(x_{t-1}|x_t, x_0) = \frac{q(x_t|x_{t-1}, x_0)q(x_{t-1}|x_0)}{q(x_t|x_0)} = \frac{(\mathbf{x}_t^T Q_t \mathbf{x}_{t-1})(\mathbf{x}_{t-1}^T \bar{Q}_{t-1} \mathbf{x}_0)}{\mathbf{x}_t^T \bar{Q}_t \mathbf{x}_0}, \quad (7)$$

thus we train a denoising model  $p_\theta(x_{t-1}|x_t, c)$  to approximate the tractable distribution  $q(x_{t-1}|x_t, x_0)$ , where  $c$  is the conditional feature of gloss sequence. And the model is trained to minimize the variational lower bound [36]:

$$\mathcal{L}_{vb} = \mathbb{E}_q \left[ \underbrace{D_{\text{KL}}(q(x_T|x_0) \parallel p_\theta(x_T))}_{L_T} - \underbrace{\log p_\theta(x_0|x_1, c)}_{L_0} \right] + \sum_{t=2}^T \underbrace{D_{\text{KL}}(q(x_{t-1}|x_t, x_0) \parallel p_\theta(x_{t-1}|x_t, c))}_{L_{t-1}}. \quad (8)$$

**Reparameterization Trick on Model Learning.** Compared with directly predicting  $p_\theta(x_{t-1}|x_t, c)$ , recent works [15, 16, 18] find that predict the data  $x_0$  gives better quality at every reverse step. Thus, we let our denoising model predict the distribution  $p_\theta(\tilde{x}_0|x_t, c)$ . With a reparameterization trick, the conditional reverse distribution can be formulated as follows:

$$p_\theta(x_{t-1}|x_t, c) = \sum_{\tilde{x}_0=1}^V q(x_{t-1}|x_t, \tilde{x}_0) p_\theta(\tilde{x}_0|x_t, c). \quad (9)$$

Under this  $x_0$ -parameterization trick, we introduce an auxiliary denoising objective to encourage good predictions

of the data  $x_0$  at each time step [2]. The final loss function is combined with the negative variational lower bound and the auxiliary loss:

$$\mathcal{L}_{\text{ddm}} = \mathcal{L}_{vb} - \lambda \log p_\theta(x_0|x_t, c), \quad (10)$$

where  $\lambda$  is a coefficient for the auxiliary loss term.

**CodeUnet for Model Learning.** Most image diffusion models [10, 16, 37] adopt the Unet [30] as their architectures since it is effective for data with spatial structure. However, directly applying the Unet in discrete sequence generation, *e.g.*, text generation [2] and quantized image synthesis [15], will bring information leakage problem since the convolution layer over adjacent tokens may provide shortcuts for the mask-based prediction [25]. Therefore, Austin *et al.* [2] and Gu *et al* [15] used the token-wise Transformer framework to learn the distribution  $p_\theta(\tilde{x}_0|x_t, c)$ . In this work, to incorporate the advantages of Unet and Transformer networks, we propose a novel architecture, CodeUnet, to learn the spatial-temporal interaction for our quantized pose sequence generation.

As shown in Figure 3, the CodeUnet consists of a contracting path (left side), an expansive path (right side), and a middle module. The middle module is an encoder-decoder Transformer framework. The encoder consists of 6 Transformer blocks. It takes the gloss sentence as input and obtains a conditional feature sequence. The decoder has two blocks. Each block has a self-attention, a cross-attention, a feed-forward network, and an Adaptive Layer Normalization (AdaLN) [3, 15]. The AdaLN operator is devised to incorporate timestep  $t$  information as  $\text{AdaLN}(h, t) = \alpha_t \text{LayerNorm}(h) + \beta_t$ , where  $h$  is the intermediate activations,  $\alpha_t$  and  $\beta_t$  are obtained from a linear projection of the timestep embedding.

The contracting and expansive paths are hierarchical structures, and each level has two Transformer encoder blocks. For downsampling in contracting path, given the feature of quantized pose sequence, *e.g.*,  $h \in \mathbb{R}^{N \times 3 \times d_{\text{model}}}$ , where  $d_{\text{model}}$  is the feature dimension, we first sample uniformly with stride 2 in the temporal dimension and remain constant in the spatial dimension. Then we set the downsampled feature as query  $Q \in \mathbb{R}^{N/2 \times 3 \times d_{\text{model}}}$ , and keep key  $K$  and value  $V$  unchanged for the following attention network. In the upsampling of the expansive path, we directly repeat the feature 2 times as a query, but the key and value remain for the following attention network:

$$\forall n = 1, \dots, N, Q_n^{\text{up}} = h_{n/2}, K^{\text{up}} = V^{\text{up}} = h, \quad (11)$$

where  $\cdot // \cdot$  denotes floor division. Finally, a linear layer and a softmax layer are applied to make the prediction.

### 3.3. Length Prediction with Sequential-KNN

In this section, inspired by [45], which merges tokens with similar semantic meanings from different locations, we

Method	WER	BLEU-1	BLEU-2	BLEU-3	BLEU-4	DTW-MJE
PTR <sup>†</sup> [33]	94.65	11.45	7.08	5.08	4.04	0.191
NAT-AT [20]	88.15	14.26	9.93	7.11	5.53	0.177
NAT-EA [20]	82.01	15.12	10.45	7.99	6.66	0.146
<b>PoseVQ-AR (Ours)</b>	85.27	14.26	10.02	7.57	5.94	0.172
<b>PoseVQ-MP (Ours)</b>	79.38	15.43	10.69	8.26	6.98	0.146
<b>PoseVQ-Diffusion (Ours)</b>	<b>77.26</b>	<b>16.11</b>	<b>11.37</b>	<b>9.22</b>	<b>7.50</b>	<b>0.116</b>
GT	50.23	23.47	15.86	12.03	10.47	0.0

Table 1. Quantitative results for the G2P task on the RWTH-PHOENIX-WEATHER-2014T test dataset. <sup>†</sup> indicates the results is provided by Huang et al. [20].

propose a novel clustering algorithm to get the lengths for corresponding glosses. Specifically, given a token sequence that is obtained from the Pose-VQVAE model, we compute the local density  $\rho$  of each token according to its  $k$ -nearest-neighbors:

$$\rho_i = \exp\left(-\frac{1}{k} \sum_{z_j \in \text{KNN}(z_i)} \|z_i - z_j\|_2^2\right), \text{ where } |i - j| \leq l \quad (12)$$

where  $i, j$  is the position in the sequence, and  $l$  is a predefined hyperparameter indicating that we only consider the local region since the adjacent tokens are more likely to belong to a gloss.  $z_i$  and  $z_j$  are the latent feature for  $i^{th}$  and  $j^{th}$  tokens.  $\text{KNN}(z_i)$  represents the  $k$ -nearest neighbors for  $i^{th}$  token.

We assign  $\{p_1, \dots, p_M\}$  positions with a higher local density as the peaks, where  $M$  is the length of the gloss sequence. Then between two adjacent peaks, for example,  $p_1$  and  $p_2$ , we sequentially iterate from  $p_1$  to  $p_2$  and find the first position that is farther from  $z_{p_1}$  and closer to  $z_{p_2}$ , which is the boundary we determined. After finding these boundaries, we get the lengths of the contiguous pose sequence for its corresponding glosses. As shown in Figure 3, we define the obtained lengths as  $\{L_1, \dots, L_M\}$ , and the Transformer encoder for gloss sequence is trained under the supervised information of lengths. For each gloss word, we predict a number from  $[1, P]$ , where  $P$  is the maximum length of the target pose sequence. Mathematically, we formulate the classification loss of length prediction as:

$$\mathcal{L}_{\text{len}} = \frac{\delta}{M} \sum_i^M \sum_j^P (-L_i = j) \log p(L_i | c). \quad (13)$$

In the training of the discrete diffusion mode,  $\mathcal{L}_{\text{len}}$  is trained together with a coefficient  $\delta$ . In the inference, we predict the length of glosses, and their summation is the length of the target pose sequence.

In summary, we arrive at our proposed two-stage approach, PoseVQ-Diffusion, with the first-stage Pose-VQVAE model and the second-stage discrete diffusion model with a length predictor.

## 4. Experiments

**Datasets.** We evaluate our G2P model on RWTH-PHOENIX-WEATHER-2014T dataset [5]. It is the *only* publicly available SLP dataset with parallel sign language videos, gloss annotations, and spoken language translations. This corpus contains 7,096 training samples (with 1,066 different sign glosses in gloss annotations and 2,887 words in German spoken language translations), 519 validation samples, and 642 test samples.

**Evaluation Metrics.** Following the widely-used setting in SLP [33], we adopt the back-translation method for evaluation. Specifically, we utilize the state-of-the-art SLT [7] model to translate the generated sign pose sequence back to gloss sequence and spoken language, where its input is modified as pose sequence. Specifically, we compute BLEU [27] and Word Error Rate (WER) between the back-translated spoken language translations and gloss recognition results with ground truth spoken language and gloss sequence.

**Data Processing.** Since the RWTH-PHOENIX-WEATHER-2014T dataset does not contain pose information, we generate the pose sequence as the ground truth. Following B. Saunders *et al.* [33], we extract 2D joint points from sign video using OpenPose [8] and lift the 2D joints to 3D with a skeletal model estimation improvement method [44]. Finally, similar to [38], we apply skeleton normalization to remove the skeleton size difference between different signers.

**Model Settings.** The Pose-VQVAE consists of an Encoder, a Tokenizer, and a Decoder. The Encoder contains a linear layer to transform pose points to a hidden feature with a dimension set as 256, a 3-layer Transformer module with divided space-time attention [4]. The Tokenizer maintains a codebook with a size set as 2,048. The Decoder contains the same 3-layer Transformer module as the Encoder and an SPL layer to predict the structural sign skeleton. For the discrete diffusion model, we set the timestep  $T$  as 100. All Transformer blocks of CodeUnet have  $d_{\text{model}}=512$  and  $N_{\text{depth}}=2$ . The size of the local region  $l$  in Eq. (12), is set as 16, which is the average length of a gloss. And the number of nearest neighbors  $k$  is set as 16. We train the model on 8 NVIDIA Tesla V100 GPUs. We include all hyperparameters settings and the details of implementation in the Appendix.

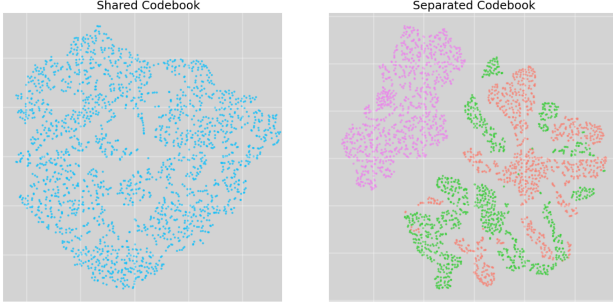


Figure 4. Visualization of latent vectors in the shared codebook and separated codebooks. In the shared codebook, all points feature to share the same latent embedding space. In the separated codebook, the latent vectors for the pose, right-hand, and left-hand are maintained in separated embedding space, where the pink part is for the pose, and the green and orange parts represent left and right hands, respectively.

#### 4.1. Comparisons with State-of-the-Art Methods

**Competing Methods.** We compare our PoseVQ-Diffusion with previous state-of-the-art G2P models. **Progressive Transformer** (PTR) [33] is the first SLP model to tackle the G2P problem in an autoregressive manner. Since they use the ground-truth first sign pose frame and timing information, their reported results are not comparable to ours. Thus we adopt the results reported by Huang *et al.* [20]. **NAT-EA** [20] proposes a non-autoregressive method to directly predict the target pose sequence with the External Aligner (EA) to learn alignments between glosses and pose sequences. **NAT-AT** is the NAT model without EA that uses the decoder-to-encoder attention to learn the alignments.

**Quantitative Comparison.** The comparison between our PoseVQ-Diffusion and the competing methods is shown in Table 1. The row of **PoseVQ-AR** refs to the vector quantized model with an autoregressive decoder. The row of **PoseVQ-MP** refs to the vector quantized model with the Mask-Predict [13] strategy, which is also a variant of discrete diffusion model [2]. **PoseVQ-Diffusion** refs to the vector quantized model with mask-and-replace diffusion strategy. As indicated in Table 1, both diffusion-based models outperform the state-of-the-art G2P models with relative improvements on WER score by 5.7% (82.01  $\rightarrow$  77.26) and on BLEU-4 by 12.6% (6.66  $\rightarrow$  7.50). This shows the effectiveness of the iterative mask-based non-autoregressive method on the vector quantized pose sequence. In addition, the Mask-Predict strategy is a mask-only strategy similar to PoseVQ-Diffusion with  $\gamma_T = 1$ . Therefore, PoseVQ-Diffusion achieves better performance than PoseVQ-MP. This reflects that the mask-and-replace strategy is superior to the mask-only strategy.

#### 4.2. Model Analysis and Discussions

We also investigate the effects of different components and design choices of our proposed model.

local patches	codebook (size)	MSE ( $\downarrow$ )	WER ( $\downarrow$ )
joint	shared (2048)	0.0242	-
separated	shared (2048)	0.0139	78.21
separated	shared (3072)	0.0131	78.15
separated	separated (1024*3)	<b>0.0113</b>	<b>77.26</b>

Table 2. Ablation on the design of Pose-VQVAE reconstruction model.

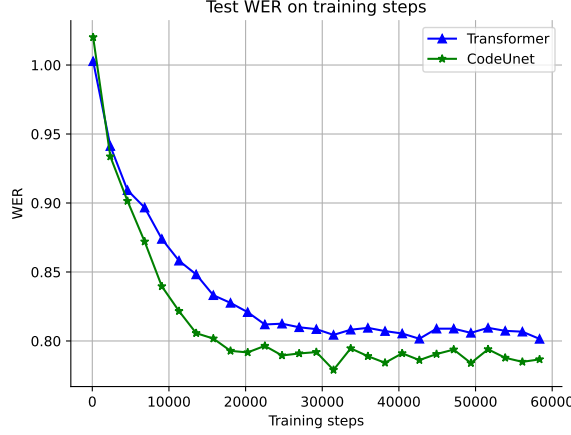


Figure 5. Ablation on the design of prediction model.

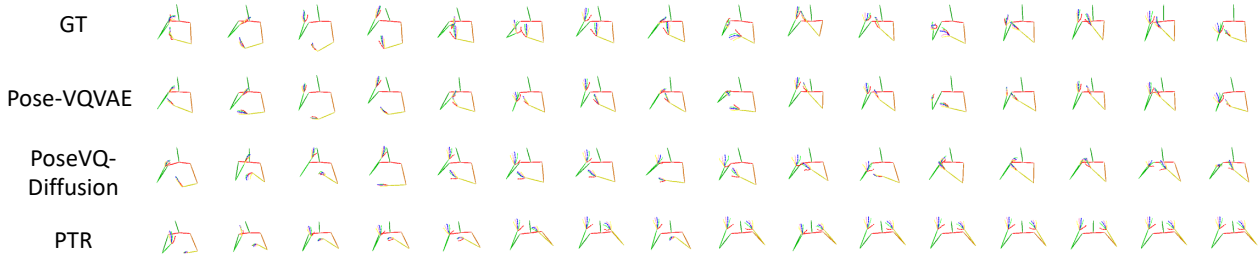
Infer. Steps	Training Steps				
	20	50	100	200	
20	79.53	79.40	78.25	78.62	
50	-	79.31	77.69	78.23	
100	-	-	<b>77.26</b>	78.18	
200	-	-	-	78.15	

Table 3. Ablation on training steps and inference steps.

**Analysis of The Design of Pose-VQVAE.** As shown in Table 2, we study the design of our Pose-VQVAE model. Pose-VQVAE-joint-shared means we compress all points into one token with one shared codebook. Pose-VQVAE-separated-shared means the points are separated into three local patches according to the structure of a sign skeleton, and the latent embedding space is maintained with one shared codebook. Pose-VQVAE-separated-separated means the points are separated into three local patches, and the latent vectors are maintained with three codebooks separately.

Experimental results in Table 2 show that Pose-VQVAE-separated-separated achieves much better reconstruction (MSE) performance. This indicates that compressing all skeleton points into one token embedding is not advisable, leading to information loss. And using separated latent feature spaces for different local regions, that is, three codebooks can achieve better reconstruction quality and generation performance. To further explain this phenomenon, we visualize the latent space vectors of shared codebooks and separated codebooks with T-SNE [40]. As shown in Figure 4, the latent space vectors corresponding to the left-hand and right-hand local regions are easily confused because of their close distances. Therefore, separated codebooks can

Sign Gloss: BESONDERS OST DEUTSCH LAND MEHR REGEN ODER SCHNEE



Sign Gloss: DONNERSTAG SUEDOST WEITER WECHSELHAFT NORDWEST MEHR FREUNDLICH SONNE

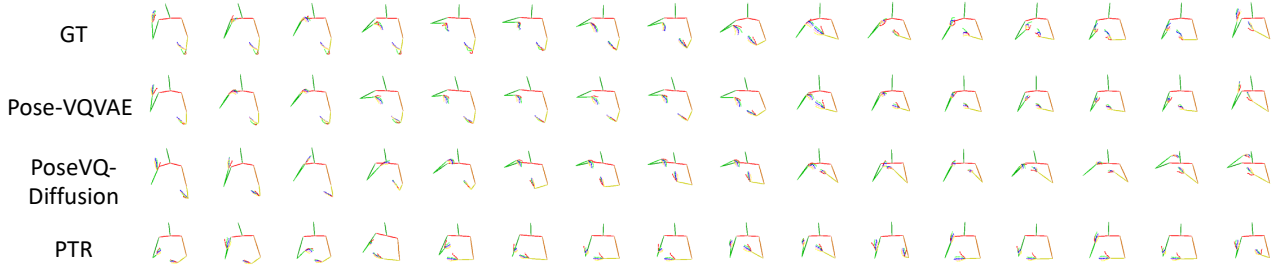


Figure 6. G2P qualitative results. We show several examples of predicted sign pose sequences compared with our reconstruction model and previous G2P model [33]. For readability, we sampled every 5 frames for a total of 16 frames. See the Appendix for more results.

reduce the difficulty in constructing mappings between the sign pose feature and the codebook feature, thus learning better latent space and reconstruction quality. The second row of Figure 6 shows the sample of sign pose sequences reconstructed by Pose-VQVAE-separated-separated.

**CodeUnet vs. Transformer.** For a fair comparison, we replace our CodeUnet with a Transformer network, keeping other settings the same. As shown in Figure 5, the diffusion-based model with our CodeUnet achieves better performance on the back-translate evaluation. This phenomenon suggests that the hierarchical structure of CodeUnet makes it particularly effective for data with spatial structure. Moreover, the curve in the figure shows that CodeUnet covers faster than Transformer. Having said that, due to sign pose sequences being temporally redundant, the compression of CodeUnet in the time dimension makes it more efficient in training.

**Number of Timesteps.** We compare the performance of the model with different numbers of training steps. As shown in the left two columns of Table 3, we find that the results get better when the training step size is increased from 20 to 100. As it increased further, the results seemed to saturate. Therefore, we set the training step to 100 to trade off performance and speed. Besides, within the same training steps, increasing the number of inference steps yields better results.

**Length Candidates.** Length prediction is essential for a non-autoregressive generation. Our approach proposes a Sequential-KNN algorithm to learn the lengths for corre-

Length Candidates	1	2	3	4	Gold
WER (↓)	79.12	78.56	<b>77.26</b>	77.73	76.39

Table 4. Ablation on length candidates.

sponding glosses and then treat the length prediction as a classification problem. As shown in the right two columns in Table 4, we study the performance with different length candidates and compare it with the reference (gold) target sequence length. The results show that multiple candidates can increase performance, but too many candidates can even degrade performance.

## 5. Conclusion

We present a novel paradigm for text-based sign pose sequence generation through an iterative non-autoregressive approach. Specifically, we first devise a specific architecture Pose-VQVAE with a multi-codebook to learn semantic discrete codes by reconstruction. Then we extend the discrete diffusion method with special states to model the alignments between sign glosses and length-varied quantized code sequences. Further, a “fully transformer” network CodeUnet is proposed to model the spatial-temporal information in discrete space. Finally, we propose a sequential-KNN algorithm to learn the length of corresponding glosses and then predict the length as a classification task. Compared with previous state-of-the-art autoregressive and non-autoregressive methods, extensive experiments demonstrate the effectiveness of our proposed PoseVQ-Diffusion framework.

## 6. Broader Impact and Limitations

We develop a general paradigm for text-based pose generation in this paper. We do not foresee any negative ethical/societal impacts at this moment. Although the proposed PoseVQ-Diffusion proves effective in conditional sign pose sequence generation, we notice several limitations of our approach. (i) Since modeling in the discrete space, the generated sequence is not smooth. (ii) Our proposed two-stage models are not end-to-end and more difficult to train than previous methods. In future work, we plan to generate pose sequences in continuous space with diffusion architecture.

## References

[1] Emre Aksan, Manuel Kaufmann, and Otmar Hilliges. Structured prediction helps 3d human motion modelling. In *2019 IEEE/CVF International Conference on Computer Vision, ICCV 2019, Seoul, Korea (South), October 27 - November 2, 2019*, pages 7143–7152. IEEE, 2019. [3](#)

[2] Jacob Austin, Daniel D. Johnson, Jonathan Ho, Daniel Tarlow, and Rianne van den Berg. Structured denoising diffusion models in discrete state-spaces. In *NeurIPS*, 2021. [2](#), [3](#), [4](#), [5](#), [7](#)

[3] Jimmy Ba, Jamie Ryan Kiros, and Geoffrey E. Hinton. Layer normalization. *ArXiv preprint*, abs/1607.06450, 2016. [5](#)

[4] Gedas Bertasius, Heng Wang, and Lorenzo Torresani. Is space-time attention all you need for video understanding? In Marina Meila and Tong Zhang, editors, *Proceedings of the 38th International Conference on Machine Learning, ICML 2021, 18-24 July 2021, Virtual Event*, volume 139 of *Proceedings of Machine Learning Research*, pages 813–824. PMLR, 2021. [6](#)

[5] Necati Cihan Camgöz, Simon Hadfield, Oscar Koller, Hermann Ney, and Richard Bowden. Neural sign language translation. In *2018 IEEE Conference on Computer Vision and Pattern Recognition, CVPR 2018, Salt Lake City, UT, USA, June 18-22, 2018*, pages 7784–7793. IEEE Computer Society, 2018. [2](#), [6](#)

[6] Necati Cihan Camgöz, Oscar Koller, Simon Hadfield, and R. Bowden. Multi-channel transformers for multi-articulatory sign language translation. *ArXiv preprint*, abs/2009.00299, 2020. [2](#)

[7] Necati Cihan Camgöz, Oscar Koller, Simon Hadfield, and Richard Bowden. Sign language transformers: Joint end-to-end sign language recognition and translation. In *2020 IEEE/CVF Conference on Computer Vision and Pattern Recognition, CVPR 2020, Seattle, WA, USA, June 13-19, 2020*, pages 10020–10030. IEEE, 2020. [2](#), [6](#)

[8] Zhe Cao, Gines Hidalgo, Tomas Simon, Shih-En Wei, and Yaser Sheikh. Openpose: Realtime multi-person 2d pose estimation using part affinity fields. *IEEE Transactions on Pattern Analysis and Machine Intelligence*, 43:172–186, 2021. [6](#)

[9] Caroline Chan, Shiry Ginosar, Tinghui Zhou, and Alexei A. Efros. Everybody dance now. In *2019 IEEE/CVF International Conference on Computer Vision, ICCV 2019, Seoul, Korea (South), October 27 - November 2, 2019*, pages 5932–5941. IEEE, 2019. [2](#)

[10] Prafulla Dhariwal and Alex Nichol. Diffusion models beat gans on image synthesis. In *NeurIPS*, 2021. [2](#), [5](#)

[11] Mingjing Du, Shifei Ding, and Hongjie Jia. Study on density peaks clustering based on k-nearest neighbors and principal component analysis. *Knowl. Based Syst.*, 99:135–145, 2016. [2](#)

[12] Patrick Esser, Robin Rombach, and Björn Ommer. Tampering transformers for high-resolution image synthesis. *2021 IEEE/CVF Conference on Computer Vision and Pattern Recognition (CVPR)*, pages 12868–12878, 2021. [2](#)

[13] Marjan Ghazvininejad, Omer Levy, Yinhan Liu, and Luke Zettlemoyer. Mask-predict: Parallel decoding of conditional masked language models. In *Proceedings of the 2019 Conference on Empirical Methods in Natural Language Processing and the 9th International Joint Conference on Natural Language Processing (EMNLP-IJCNLP)*, pages 6112–6121, Hong Kong, China, 2019. Association for Computational Linguistics. [1](#), [2](#), [7](#)

[14] Jiatao Gu, James Bradbury, Caiming Xiong, Victor O. K. Li, and Richard Socher. Non-autoregressive neural machine translation. In *6th International Conference on Learning Representations, ICLR 2018, Vancouver, BC, Canada, April 30 - May 3, 2018, Conference Track Proceedings*. OpenReview.net, 2018. [1](#)

[15] Shuyang Gu, Dong Chen, Jianmin Bao, Fang Wen, Bo Zhang, Dongdong Chen, Lu Yuan, and Baining Guo. Vector quantized diffusion model for text-to-image synthesis. *ArXiv preprint*, abs/2111.14822, 2021. [2](#), [3](#), [4](#), [5](#)

[16] Jonathan Ho, Ajay Jain, and Pieter Abbeel. Denoising diffusion probabilistic models. In Hugo Larochelle, Marc'Aurelio Ranzato, Raia Hadsell, Maria-Florina Balcan, and Hsuan-Tien Lin, editors, *Advances in Neural Information Processing Systems 33: Annual Conference on Neural Information Processing Systems 2020, NeurIPS 2020, December 6-12, 2020, virtual*, 2020. [2](#), [5](#)

[17] Jonathan Ho, Chitwan Saharia, William Chan, David Fleet, Mohammad Norouzi, and Tim Salimans. Cascaded diffusion models for high fidelity image generation. *J. Mach. Learn. Res.*, 23:47:1–47:33, 2022. [2](#)

[18] Emiel Hoogeboom, Didrik Nielsen, Priyank Jaini, Patrick Forr'e, and Max Welling. Argmax flows and multinomial diffusion: Towards non-autoregressive language models. *ArXiv preprint*, abs/2102.05379, 2021. [2](#), [5](#)

[19] Hezhen Hu, Weichao Zhao, Wen gang Zhou, Yuechen Wang, and Houqiang Li. Signbert: Pre-training of hand-model-aware representation for sign language recognition. *2021 IEEE/CVF International Conference on Computer Vision (ICCV)*, pages 11067–11076, 2021. [2](#)

[20] Wencan Huang, Wenwen Pan, Zhou Zhao, and Qi Tian. Towards fast and high-quality sign language production. *Proceedings of the 29th ACM International Conference on Multimedia*, 2021. [1](#), [2](#), [6](#), [7](#)

[21] Myeonghun Jeong, Hyeongju Kim, Sung Jun Cheon, Byoung Jin Choi, and Nam Soo Kim. Diff-tts: A denoising diffusion model for text-to-speech. In *Interspeech*, 2021. [2](#)

[22] Heeseung Kim, Sungwon Kim, and Sungroh Yoon. Guided-tts: A diffusion model for text-to-speech via classifier guidance. 2021. 2

[23] Jaehyeon Kim, Sungwon Kim, Jungil Kong, and Sungroh Yoon. Glow-tts: A generative flow for text-to-speech via monotonic alignment search. In Hugo Larochelle, Marc'Aurelio Ranzato, Raia Hadsell, Maria-Florina Balcan, and Hsuan-Tien Lin, editors, *Advances in Neural Information Processing Systems 33: Annual Conference on Neural Information Processing Systems 2020, NeurIPS 2020, December 6-12, 2020, virtual*, 2020. 2

[24] Zhifeng Kong, Wei Ping, Jiaji Huang, Kexin Zhao, and Bryan Catanzaro. Diffwave: A versatile diffusion model for audio synthesis. In *9th International Conference on Learning Representations, ICLR 2021, Virtual Event, Austria, May 3-7, 2021*. OpenReview.net, 2021. 2

[25] Piotr Nawrot, Szymon Tworkowski, Michal Tyrolski, Lukasz Kaiser, Yuhuai Wu, Christian Szegedy, and Henryk Michalewski. Hierarchical transformers are more efficient language models. *ArXiv preprint*, abs/2110.13711, 2021. 5

[26] Alexander Quinn Nichol and Prafulla Dhariwal. Improved denoising diffusion probabilistic models. In Marina Meila and Tong Zhang, editors, *Proceedings of the 38th International Conference on Machine Learning, ICML 2021, 18-24 July 2021, Virtual Event*, volume 139 of *Proceedings of Machine Learning Research*, pages 8162–8171. PMLR, 2021. 2

[27] Kishore Papineni, Salim Roukos, Todd Ward, and Wei-Jing Zhu. Bleu: a method for automatic evaluation of machine translation. In *Proceedings of the 40th Annual Meeting of the Association for Computational Linguistics*, pages 311–318, Philadelphia, Pennsylvania, USA, 2002. Association for Computational Linguistics. 6

[28] Roland Pfau, Martin Salzmann, and Markus Steinbach. The syntax of sign language agreement: Common ingredients, but unusual recipe. *Glossa: a journal of general linguistics*, 2018. 1

[29] Robin Rombach, A. Blattmann, Dominik Lorenz, Patrick Esser, and Björn Ommer. High-resolution image synthesis with latent diffusion models. *ArXiv preprint*, abs/2112.10752, 2021. 2

[30] Olaf Ronneberger, Philipp Fischer, and Thomas Brox. U-net: Convolutional networks for biomedical image segmentation. In *MICCAI*, 2015. 2, 5

[31] Ben Saunders, Richard Bowden, and Necati Cihan Camgöz. Adversarial training for multi-channel sign language production. In *31st British Machine Vision Conference 2020, BMVC 2020, Virtual Event, UK, September 7-10, 2020*. BMVA Press, 2020. 1

[32] Ben Saunders, Necati Cihan Camgoz, and R. Bowden. Everybody sign now: Translating spoken language to photo realistic sign language video. *ArXiv preprint*, abs/2011.09846, 2020. 1, 2

[33] Ben Saunders, Necati Cihan Camgöz, and R. Bowden. Progressive transformers for end-to-end sign language production. *ArXiv preprint*, abs/2004.14874, 2020. 1, 2, 6, 7, 8

[34] Ben Saunders, Necati Cihan Camgöz, and Richard Bowden. Mixed signals: Sign language production via a mixture of motion primitives. In *2021 IEEE/CVF International Conference on Computer Vision, ICCV 2021, Montreal, QC, Canada, October 10-17, 2021*, pages 1899–1909. IEEE, 2021. 2

[35] Florian Schmidt. Generalization in generation: A closer look at exposure bias. In *Proceedings of the 3rd Workshop on Neural Generation and Translation*, pages 157–167, Hong Kong, 2019. Association for Computational Linguistics. 1

[36] Jascha Sohl-Dickstein, Eric A. Weiss, Niru Maheswaranathan, and Surya Ganguli. Deep unsupervised learning using nonequilibrium thermodynamics. In Francis R. Bach and David M. Blei, editors, *Proceedings of the 32nd International Conference on Machine Learning, ICML 2015, Lille, France, 6-11 July 2015*, volume 37 of *JMLR Workshop and Conference Proceedings*, pages 2256–2265. JMLR.org, 2015. 2, 5

[37] Yang Song, Jascha Sohl-Dickstein, Diederik P. Kingma, Abhishek Kumar, Stefano Ermon, and Ben Poole. Score-based generative modeling through stochastic differential equations. In *9th International Conference on Learning Representations, ICLR 2021, Virtual Event, Austria, May 3-7, 2021*. OpenReview.net, 2021. 5

[38] Stephanie Stoll, Necati Cihan Camgöz, Simon Hadfield, and Richard Bowden. Sign language production using neural machine translation and generative adversarial networks. In *British Machine Vision Conference 2018, BMVC 2018, Newcastle, UK, September 3-6, 2018*, page 304. BMVA Press, 2018. 2, 6

[39] Aäron van den Oord, Oriol Vinyals, and Koray Kavukcuoglu. Neural discrete representation learning. In Isabelle Guyon, Ulrike von Luxburg, Samy Bengio, Hanna M. Wallach, Rob Fergus, S. V. N. Vishwanathan, and Roman Garnett, editors, *Advances in Neural Information Processing Systems 30: Annual Conference on Neural Information Processing Systems 2017, December 4-9, 2017, Long Beach, CA, USA*, pages 6306–6315, 2017. 2, 3

[40] Laurens Van der Maaten and Geoffrey Hinton. Visualizing data using t-sne. *Journal of machine learning research*, 9(11), 2008. 7

[41] Ronald J. Williams and David Zipser. A learning algorithm for continually running fully recurrent neural networks. *Neural Computation*, 1:270–280, 1989. 1

[42] Qinkun Xiao, Minying Qin, and Yuting Yin. Skeleton-based chinese sign language recognition and generation for bidirectional communication between deaf and hearing people. *Neural networks : the official journal of the International Neural Network Society*, 125:41–55, 2020. 2

[43] Pan Xie, Mengyi Zhao, and Xiaohui Hu. Pisltrc: Position-informed sign language transformer with content-aware convolution. *ArXiv preprint*, abs/2107.12600, 2021. 2

[44] Jan Zelinka and Jakub Kanis. Neural sign language synthesis: Words are our glosses. *2020 IEEE Winter Conference on Applications of Computer Vision (WACV)*, pages 3384–3392, 2020. 6

[45] Wang Zeng, Sheng Jin, Wentao Liu, Chen Qian, Ping Luo, Ouyang Wanli, and Xiaogang Wang. Not all tokens are equal: Human-centric visual analysis via token clustering transformer. *ArXiv preprint*, abs/2204.08680, 2022. 2, 5

[46] Hao Zhou, Wen gang Zhou, Yun Zhou, and Houqiang Li. Spatial-temporal multi-cue network for sign language recognition and translation. *IEEE Transactions on Multimedia*, 24:768–779, 2022. [2](#)